

## Amorphization in quenched ice VIII: A first-principles study

Koichiro Umemoto and Renata M. Wentzcovitch\*

*Department of Chemical Engineering and Materials Science and Minnesota Supercomputing Institute, University of Minnesota,  
421 Washington Avenue SE, Minneapolis, Minnesota 55455, USA*

(Received 2 February 2004; published 17 May 2004)

Ice VIII is a high-density form of H<sub>2</sub>O that amorphizes upon heating after being decompressed to 0 kbar. Here we investigate by first principles the structural and vibrational properties of ice VIII under decompression. We have reproduced the peculiar nonlinear behavior of some stretching and translational modes under decompression and relate this behavior to the eminent collapse of the hydrogen-bond networks. We also find that the transverse acoustic phonon branches almost collapse and are nearly unstable at 0 kbar. This is the sign of imminent amorphization, similar to that uncovered in  $\alpha$ -quartz under pressure near the amorphous transition. By means of quasi-harmonic free energy calculations we also investigate its thermal equation of state and show, for the first time, the effect of zero point motion and temperature on its structure. The level of agreement between theoretical and experimental results is unprecedented in this class of materials. This is crucial to clarifying the relationship between amorphization and acoustic phonon collapse.

DOI: 10.1103/PhysRevB.69.180103

PACS number(s): 64.70.Rh, 63.20.Dj, 83.80.Nb

Pressure-induced amorphization is one of the intriguing facts common to H<sub>2</sub>O-ice and silica. It was first observed in ordinary ice Ih under pressure at 77 K,<sup>1</sup> but has been more extensively investigated in  $\alpha$ -quartz at room temperature.<sup>2</sup> Despite all progress and efforts to understand amorphization, a consensus has not been reached yet about its root cause. Here we investigate by first principles a phenomenon that has been proposed to cause amorphization in  $\alpha$ -quartz and has not been demonstrated yet in any system that amorphizes other than  $\alpha$ -quartz: acoustic phonon collapse, i.e., the instability of entire acoustic branches,<sup>3,4</sup> or nearly so. The relationship between this phenomenon and amorphization is clearly demonstrated in this study of the structural, mechanical, and vibrational properties of ice VIII under decompression. This is a quenchable high-pressure phase of ice that upon heating to  $\sim 130$  K at 0 kbar undergoes amorphization.<sup>5</sup>

H<sub>2</sub>O-ice is a notorious material for which the predictive limits of theoretical approaches are still being explored. Experimental challenges posed by low temperatures, low scattering power of protons, or difficulties in locating phase boundaries also conspire to make comparisons with experiments nontrivial. Much has been learned about ice physics by means of model potential calculations<sup>6</sup> and, more recently, also by first-principles methods.<sup>7,8</sup> In general, model potential studies have been more complex at the expense of being less predictive. Amorphization in ice Ih and VIII has already been investigated using the model potential.<sup>6</sup> However, a question as delicate as this should always be approached with maximum precaution, and be investigated by first principles to the extent it is possible. Particularly in ice, effects related to quantum fluctuation of protons, anharmonicities, and unsatisfactory description of the hydrogen bond within density functional theory (DFT)<sup>9</sup> are expected to be non-negligible. Considering these facts, ice VIII is perhaps the least problematic system for investigating amorphization. Its structural and vibrational behavior under decompression have been partially, but carefully, characterized.<sup>7,10</sup> It has a small primitive cell (bct with space group  $I4_1/amd$ ) with

only four molecules and, because it is a denser form of ice, a DFT based approach is likely to be more successful than for the low-pressure phases.

Our static calculations of internal energies, elastic constants, and phonon frequencies use the same approaches already tested in our previous study of ice XI,<sup>11</sup> differing only in some structure-dependent details (see Ref. 11). Throughout the relevant range of volumes, static elastic moduli and Born stability criteria are also obtained from stress-strain relations, and full phonon dispersions are obtained to analyze the relationship between elastic and vibrational instabilities. In possession of the vibrational density of states we are able to calculate free energies<sup>12</sup> within the quasiharmonic approximation<sup>13</sup> to investigate the effects of zero point motion (ZPM) and temperature on the structure and equation of state of ice VIII. Effects of quantum fluctuations on the ice VIII-to-X transition pressure have been previously investigated,<sup>8</sup> however, ZPM and thermal effects on the structure and equation of state parameters are calculated here for the first time.

The robust high- $P$ /low- $T$  ice VIII phase is stable in a relatively wide range of pressures (from  $\sim 20$  to  $\sim 800$  kbar). Its high- $T$  form, ice VII, is hydrogen-disordered and stable in a similar pressure range. Both consist of two interpenetrating hydrogen-bond networks, each one containing oxygens at the sites of a diamond lattice. Ice VIII is antiferroelectric with dipole moments oriented in opposite directions in each network. Ice VII is paraelectric with randomly oriented moments. This structural type, often referred to as a self-clathrate, contrasts sharply with those of the zero pressure phases that consist of single hydrogen-bond networks. Hydrogen-disordered ice Ih, the low- $P$ /high- $T$  form, and hydrogen-ordered ice XI, its low- $T$  version, consist of a single hexagonal-diamond lattice of oxygens, being paraelectric and ferroelectric, respectively. Metastable, hydrogen-disordered ice Ic is the cubic diamond version of ice Ih and the single network version of ice VII. A first-principles description of the hydrogen bond is anticipated to be tricky. The bond charge is low, the bond is highly com-

TABLE I. Lattice constants, bond lengths, and equation of state parameters of ice VIII at two pressures, 0 and 24 kbar, and various temperatures. O-H and O $\cdots$ H are intramolecular and hydrogen-bond lengths, respectively. O-O and O $\cdots$ O are the distances between nearest oxygens connected or not by hydrogen bonds, respectively.

	$T$ (K)	$P$ (kbar)	$a$ (Å)	$c$ (Å)	O-H (Å)	O $\cdots$ H (Å)	O-O (Å)	O $\cdots$ O (Å)	$V$ (Å <sup>3</sup> )	$B_0$ (GPa)	$B'_0$
Calc. <sup>a</sup>	0	0	4.813	6.950	0.985	1.984	2.968	2.844	80.49	20.09	5.01
Calc. <sup>a</sup>	0+ZPM	0	4.905	7.095	0.982	2.045	3.027	2.890	85.34	15.91	4.95
Calc. <sup>a</sup>	85	0	4.911	7.105	0.982	2.049	3.030	2.894	85.67	15.53	4.98
Expt. <sup>b</sup>	85	0	...	...	...	...	...	...	79.97	23.8	4.5
Calc. <sup>b</sup>	0	24	4.685	6.710	0.987	1.883	2.870	2.760	72.80	...	...
Calc. <sup>a</sup>	0+ZPM	24	4.727	6.817	0.986	1.929	2.914	2.797	76.17	...	...
Calc. <sup>a</sup>	10	24	4.727	6.817	0.986	1.929	2.914	2.797	76.16	...	...
Expt. <sup>c</sup>	10	24	4.656	6.775	0.968	1.911	2.879	2.743	73.43	...	...

<sup>a</sup>This calculation.

<sup>b</sup>Reference 10.

<sup>c</sup>Reference 15.

pressible, and its bond length, O $\cdots$ H, is likely to be underestimated, more so using the local density approximation than the generalized gradient approximation (GGA). Table I lists equations of state (EoS) parameters (third-order finite strain), lattice parameters, and bond lengths at various temperatures and two pressures.<sup>14</sup> ZPM effects are significant and cannot be ignored. Thermal effects are small but noticeable. EoS parameters obtained in static calculations are in excellent agreement with the experimental values. After inclusion of ZPM and thermal effects, the agreement is still very good, typical of high-quality DFT calculations in “normal” materials that have included these effects.<sup>12</sup> However, the measurements cited in Table I were performed in D<sub>2</sub>O-ice VIII,<sup>10,15</sup> which should be less affected by ZPM and temperature. O-H and O $\cdots$ H are intramolecular and hydrogen-bond lengths, respectively. The slight overestimation of O-H and underestimation of O $\cdots$ H in static calculations

is consistent with other GGA results obtained in the isolated molecule<sup>7,16</sup> and in the dimer.<sup>16</sup> Because the hydrogen bond is the most compressive, it is also the most affected by ZPM and temperature. The O-H and O $\cdots$ H bond lengths change in the correct direction and agree better with measurements after inclusion of these effects. The distances between nearest oxygens connected (O-O) or not (O $\cdots$ O) through hydrogen bonds are also listed. As noticed earlier, O $\cdots$ O is shorter than O-O.<sup>15</sup> These distances are in better agreement with measurements before these corrections are included, and so does the volume. The final structural discrepancies should be viewed as the true DFT error, plus some possible anharmonic effects and intrinsic differences from D<sub>2</sub>O.

Good agreement between our results and experimental data<sup>10,15</sup> at two pressures is reassuring. However, some unusual structural/vibrational features in D<sub>2</sub>O-ice VIII have

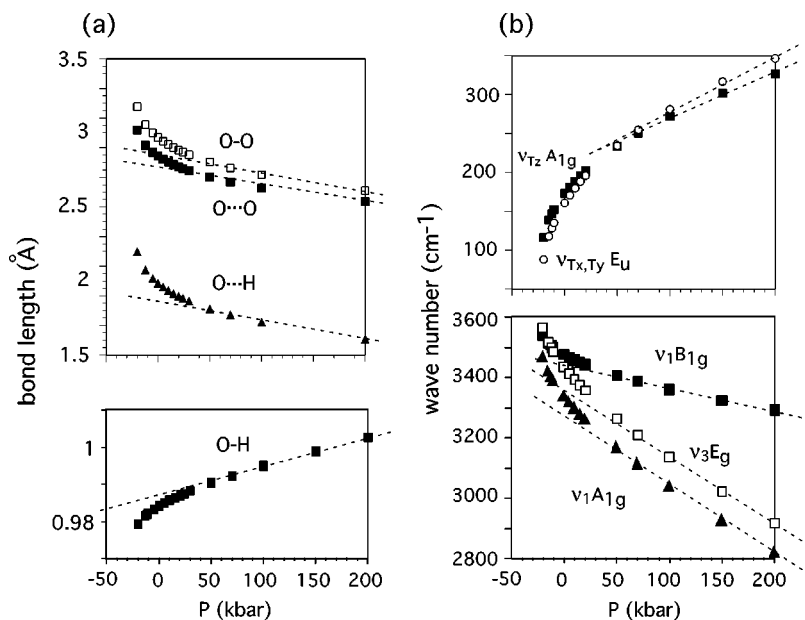


FIG. 1. Calculated (static) pressure dependence of (a) various bond lengths (see the text) related to (b) translational IR-active ( $\nu_{T_x, T_y} E_u$ ), IR-inactive ( $\nu_{T_z} A_{1g}$ ), and three Raman-active O-H stretching mode frequencies ( $\nu_1 A_{1g}$ ,  $\nu_3 E_g$ ,  $\nu_1 B_{1g}$ ).

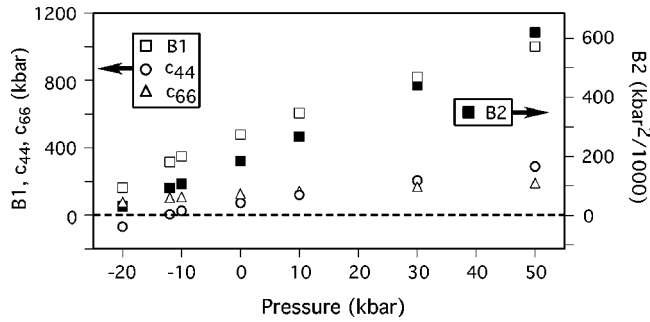


FIG. 2. Static pressure dependence of Born stability criteria. B1 and B2 are  $c_{11} - |c_{12}|$  and  $(c_{11} + c_{12})c_{33} - 2c_{13}^2$ , respectively.

been noticed and carefully documented. Their reproducibility by any theoretical approach is another crucial test. It was pointed out that extrapolation to low  $P$ 's of three Raman-active O-H stretching and one IR-active translation mode frequencies obtained at high pressures did not agree with low-pressure measurements (Whether these frequencies vary continuously or not throughout the entire pressure range has remained an open question).<sup>10</sup> Neutron diffraction determination of structural parameters within the same pressure interval suggested the structure could be relaxing discontinuously, i.e., undergoing an iso-symmetric transformation.<sup>10</sup> Here we inspect the behavior of these modes and related bond lengths (cited in Table I) under decompression. Figure 1(b) indicates the behavior observed in  $D_2O$ <sup>10</sup> is well reproduced with no observed discontinuities.  $\nu_1 A_{1g}$ ,  $\nu_1 B_{1g}$ , and  $\nu_3 E_g$  shown in the lower panel 1(b), are the stretching mode frequencies related primarily with the intramolecular bond length shown in the lower panel 1(a). The crossing of  $\nu_1 B_{1g}$  and  $\nu_3 E_g$  at low pressure<sup>10</sup> is particularly well reproduced.  $\nu_{Tz} A_{1g}$  and  $\nu_{Tx, Ty} E_u$  shown in the upper panel 1(b) are translational mode frequencies that depend on the stiffness of the intermolecular bonds shown in the upper panel 1(a). As the structure decompresses, hydrogen bonds (O $\cdots$ H) stretch and weaken, first linearly with pressure, but then the behavior becomes highly nonlinear at low  $P$ 's. The intramolecular bond behaves oppositely. Despite these nonlinearities, all quantities vary smoothly. The more rapid shortening of the O-H and lengthening of O $\cdots$ H, O $\cdots$ O, and O-O bonds is a

sign of the imminent collapse of the two hydrogen-bond networks. However, their reconstruction into a single one with shorter hydrogen bonds is not accomplished without annealing at 0 kbar. First, it undergoes amorphization upon heating to 130 K,<sup>5</sup> then it goes through metastable ice Ic, the first accessible (hydrogen-disordered) single network structure, at  $\sim 150$  K. Finally it reaches stable ice Ih at  $\sim 210$  K,<sup>5</sup> all at 0 kbar. Temperature should also aid the entropic stabilization of these disordered phases, but that might not be its primary role.

With this picture in mind we now inspect the Born criteria for mechanical stability and the phonon dispersions of ice VIII under decompression. Figure 2 displays the former obtained in static 0 K calculations. All Born coefficients decrease with pressure but the first one to vanish at “ $-12$  kbar” ( $-4.5$  kbar after ZPM corrections are considered) is  $c_{44}$ . This result is consistent with the observation of metastable ice VIII at 0 kbar. However, it also shows that ice VIII is well *on the path* leading to a mechanical instability.  $c_{44}$  determines the restoring force for the long wavelengths degenerate transverse acoustic (TA) modes propagating in the  $z$  direction (with strain  $\epsilon_4 = \epsilon_5$  in Voigt's notation<sup>17</sup>). The pressure dependence of these TA branches is displayed in Fig. 3. At “ $-12$  kbar” the entire branches become unstable along the  $\Lambda$  line at once. In ice VIII, *acoustic phonon collapse* is unambiguously linked to the mechanical instability through  $c_{44}$ .

The current study points to the importance of having the experimental facts related to amorphization clearly documented and well reproduced theoretically before they can be interpreted and conclusions are attempted. Amorphization in ice VIII is a particularly neat case because it has a unique hydrogen-bond length and, under decompression, they all collapse at the same pressure (negative one in this case). All TA normal modes along the  $\Lambda$  line involve hydrogen-bond stretching, some more, some less, depending on the wave number. Therefore, the concurrent instability of all phonons in these branches can be attributed to the critical stretching of the same bond at the critical pressure (at 0 K). Most important, these modes are not unstable as the pressure amorphization occurs experimentally. Ice VIII is mechanically and vibrationally stable at 0 kbar. However, all these phonons are

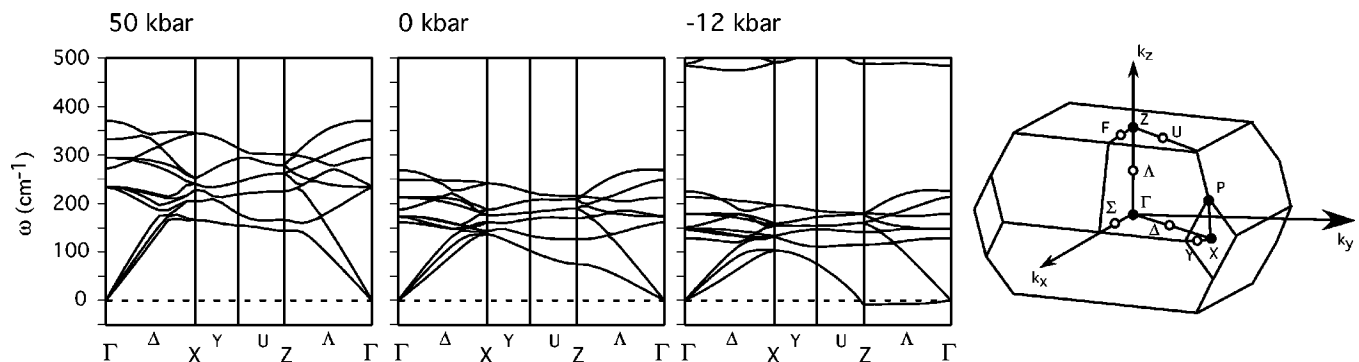


FIG. 3. Dispersions of translational modes at 50, 0, and  $-12$  kbar (static values). After inclusion of zero point motion, pressures at the same volumes are 65, 10, and  $-4.5$  kbar. Negative wavenumbers are actually imaginary numbers. On the right, the Brillouin zone of the body-centered tetragonal lattice is shown.

thermally excited simultaneously when the amorphous is produced, the first accessible metastable phase.<sup>3</sup> At 0 kbar, this happens at 130 K ( $\sim 11$  meV), while the energies of these phonons lie within  $\sim 10$  meV. This phenomenon can look more complicated in other molecular phases of ice where there is more than one hydrogen-bond length, resulting in acoustic phonon dispersions not as simple as in ice VIII.<sup>11</sup> For instance, an intermediate phase has been observed in  $\alpha$ -quartz before amorphization,<sup>2</sup> most likely as a result of an acoustic phonon collapse starting at the Brillouin zone edge.<sup>18</sup> Conceivably, nonuniform or nonhydrostatic pressures could have a similarly complicating effect by alter-

ing bond lengths nonuniformly. In any case, it is the collapse of the two hydrogen-bond networks and their nontrivial reconstruction into a single one that is behind amorphization in ice VIII.

We thank S. Baroni for fruitful discussions. Calculations have been performed using the PWscf package <http://www.pwscf.org>. This research was supported by NSF Grants Nos. EAR-0135533 (COMPRES) and EAR-0230319. Computations were performed at the Minnesota Supercomputing Institute.

\*Electronic address: wentzcov@cems.umn.edu

<sup>1</sup>O. Mishima, L.D. Calvert, and E. Whalley, *Nature (London)* **310**, 393 (1984).

<sup>2</sup>K.J. Kingma, C. Meade, R.J. Hemley, H.K. Mao, and D.R. Veblen, *Science* **259**, 666 (1993); K.J. Kingma, R.J. Hemley, H.K. Mao, and D.R. Veblen, *Phys. Rev. Lett.* **70**, 3927 (1993).

<sup>3</sup>S.L. Chaplot and S.K. Sikka, *Phys. Rev. Lett.* **71**, 2674 (1993); N. Binggeli and J.R. Chelikowsky, *ibid.* **71**, 2675 (1993).

<sup>4</sup>S. Baroni and P. Giannozzi, in *High-Pressure Materials Research Symposium, Boston, MA, 1997* edited by R.M. Wentzcovitch, R. Hemley, and W. Nellis, *Mater. Res. Soc. Symp. Proc.* **499**, 233 (1998).

<sup>5</sup>D.D. Klug, Y.P. Handa, J.S. Tse, and E. Whalley, *J. Chem. Phys.* **90**, 2390 (1989); A.M. Balagurov, O.I. Barkalov, A.I. Kolesnikov, G.M. Mironova, E.G. Ponyatovskii, V.V. Sinitsyn, and V.K. Fedotov, *JETP Lett.* **53**, 30 (1991).

<sup>6</sup>J.S. Tse, *J. Chem. Phys.* **96**, 5482 (1992); J.S. Tse, V.P. Shpakov, and V.R. Belosludov, *ibid.* **111**, 11111 (1999).

<sup>7</sup>J.S. Tse and D.D. Klug, *Phys. Rev. Lett.* **81**, 2466 (1998).

<sup>8</sup>M. Benoit, D. Marx, and M. Parrinello, *Nature (London)* **392**, 258 (1998); *Comput. Mater. Sci.* **10**, 88 (1998).

<sup>9</sup>P. Hohenberg and W. Kohn, *Phys. Rev.* **136**, B864 (1964); W. Kohn and L.J. Sham, *Phys. Rev.* **140**, A1133 (1965).

<sup>10</sup>J.M. Besson, S. Klotz, G. Hamel, W.G. Marshall, R.J. Nelmes, and J.S. Loveday, *Phys. Rev. Lett.* **78**, 3141 (1997).

<sup>11</sup>K. Umemoto, R.M. Wentzcovitch, S. Baroni, and S. de Gironcoli, *Phys. Rev. Lett.* **92**, 105502 (2004). We have used norm-conserving pseudopotentials [N. Troullier and J.L. Martins, *Phys. Rev. B* **43**, 1993 (1991)] with a plane-wave cutoff of 100 Ry, generalized gradient approximation for the exchange correlation functional [J.P. Perdew, K. Burke, and M. Ernzerhof,

*Phys. Rev. Lett.* **77**, 3865 (1996)], density-functional perturbation theory for phonon calculations [S. Baroni, S. de Gironcoli, A. Dal Corso, and P. Giannozzi, *Rev. Mod. Phys.* **73**, 515 (2001)], and the variable-cell-shape dynamics for structural optimizations [R.M. Wentzcovitch, *Phys. Rev. B* **44**, 2358 (1991)]. The number of  $\mathbf{k}$ -points in the irreducible wedge of the undistorted Brillouin Zone is eleven.

<sup>12</sup>B.B. Karki, R.M. Wentzcovitch, S. de Gironcoli, and S. Baroni, *Phys. Rev. B* **62**, 14750 (2000); *Science* **286**, 1705 (1999).

<sup>13</sup>D. Wallace, *Thermodynamics of Crystals* (Wiley, New York, 1972).

<sup>14</sup>The estimation of structural parameters at high  $T$  was done by invoking a corollary of the QHA (Ref. 13): in this approximation structural parameters and phonon frequencies are those obtained in static  $T=0$  K calculations and depend on volume alone. Within the  $(P, T)$  range of validity of this approximation, if two states  $(P, T)$  and  $(P', T')$  have the same volume, their structural parameters and phonon spectra must be equal. Therefore, the  $T$  dependence of structural parameters occurs via volume only. This estimation should be more accurate at higher  $P$  and lower  $T$  than at lower  $P$  and higher  $T$ . In the latter case, anharmonic effects might be non-negligible and the QHA could overestimate these effects. In either case their magnitudes are similar.

<sup>15</sup>W.F. Kuhs, J.L. Finney, C. Vettier, and D.V. Bliss, *J. Chem. Phys.* **81**, 3612 (1984).

<sup>16</sup>K. Laasonen, F. Csajka, and M. Parrinello, *Chem. Phys. Lett.* **194**, 172 (1992).

<sup>17</sup>M. Born and K. Huang, *Dynamical Theory of Crystal Lattices* (Clarendon, Oxford, 1954), Sec. 11.

<sup>18</sup>R.M. Wentzcovitch, C. da Silva, J.R. Chelikowsky, and N. Binggeli, *Phys. Rev. Lett.* **80**, 2149 (1998).